Unified Treatment of Flow Instabilities of Turbomachines

Y. Tsujimoto, K. Kamijo, C. E. Brennen

Unified Treatment of Flow Instabilities of Turbomachines

Yoshinobu Tsujimoto*
Osaka University, Osaka 560-8531, Japan
Kenjiro Kamijo†
Tohoku University, Sendai, Miyagi 980-8577, Japan
and
Christopher E. Brennen‡
California Institute of Technology, Pasadena, California 91125

The relationship among four flow instabilities of turbomachines, namely, surge, rotating stall, cavitation surge, and rotating cavitation, is elucidated, using a unified or common model for their analysis. The simplest unifying model was employed in the analysis to focus on the characteristic features of each instability. Moreover, the concentration is on the stability criteria, and hence, the amplitudes are assumed small. Of course, the instabilities often grow to amplitudes comparable with the average value of the flow variable. Flows upstream and downstream of the impeller were assumed to be one dimensional for surge and cavitation surge and to be two dimensional for rotating stall and rotating cavitation, respectively. Viscous effects were taken into consideration in the form of cascade loss. Impeller blade geometry was incorporated in the assumption that the flow is perfectly guided. The peripheral wavelength of the disturbance was assumed to be much larger than the blade pitch.

Nomenclature

A	=	cross-sectional area of tank
a	=	nondimensional cavity volume
B	=	Greitzer's B factor
C	=	compliance
$F_{1,2,3}$	=	cavitation characteristics in Eq. (10′)
h	=	blade spacing
j	=	imaginary unit
K	=	cavitation compliance
k	=	reduced frequency, $sn/U = k_R + jk_I$
k_L	=	reduced frequency, $2\pi nL/U$
L	=	inlet conduit length
ℓ	=	chord length
M	=	mass flow gain factor
n	=	complex frequency
p	=	pressure
p_{t1}	=	inlet total pressure
p_v	=	vapor pressure
s	=	wavelength of disturbances
t	=	time
U, V	=	mean velocities in x and y directions
U_T	=	translating velocity of cascade
u, v	=	velocities in x and y directions
$\tilde{u}, \tilde{v}$	=	fluctuating velocity in x and y directions
V_c	=	cavity volume
W	=	relative velocity
α_1	=	incidence angle
β_1	=	inlet blade angle
$\bar{\beta}_1$	=	average inlet flow angle
β^*	=	average blade angle, $(\beta_1^* + \beta_2^*)/2$
β_1^*	=	inlet blade angle
β_2^*	=	outlet blade angle
ΔV	=	incident velocity
δ	=	disturbance
ζ_Q	=	through flow loss coefficient
ζ_S	=	incident flow loss coefficient
σ	=	cavitation number, $(p_1 - p_v)/(\rho W_1^2)/2)$
ϕ	=	velocity potential or flow coefficient
ψ_{ts}	=	head rise coefficient

Subscripts

1	=	upstream of impeller
2	=	downstream of impeller
3	=	downstream of tank

Introduction

IN this paper, we examine the relations between the four flow instabilities of turbomachines using a unified or common model for the flow. The instabilities that are addressed are those of surge, rotating stall, cavitation surge, and rotating cavitation.[1] Each of these are well known individually and have been subject to extensive analysis.[2-7] Our purpose is to present a unified treatment of these instabilities. One beneficial consequence of doing so is to shed light on the circumstances in which one or the other may predominate. Another benefit is the information that can be extracted from observations of one instability and used in analysis of another. For example, previous studies of surge, rotating stall, and cavitation surge were recently used by Tsujimoto et al.[8] to elucidate rotating cavitation instabilities in high-speed pumps.

Note that cavitation surge is used here to denote the phenomenon often called autooscillation in the literature. It is the opinion of the authors that cavitation surge is a more appropriate name.

The simplest model was employed in the present analysis to focus on the characteristic features of each instability. Moreover, the concentration is on the stability criteria, and hence, the amplitudes are assumed small. Of course, the instabilities often grow to large amplitudes. Although high accuracy is not expected with this method, it was very useful in both understanding and clarifying the flow instabilities of turbomachines. The following assumptions were also made: Flows upstream and downstream are one dimensional for surge and cavitation surge and are two dimensional for rotating stall and rotating cavitation, respectively. Viscous effects were taken into consideration in the form of cascade loss. Impeller blade geometry

was incorporated in the assumption that the flow is perfectly guided. The peripheral wavelength of the flow disturbance is much larger than the blade pitch.

Characteristics of Components

Flow Model

In this analysis we use the simplified fluid system shown in Fig. 1, composed of a suction conduit and a turbomachine with only a hub and rotating blades. In this section, numerical expressions are derived for each component, which are then used throughout the analysis. These components are the flow upstream of the impeller, cavitation in the pump inlet, head rise of the impeller, and the flow downstream of the impeller.

Flow Upstream of the Impeller

Rotating Stall Case and Rotating Cavitation Case (Two-Dimensional Instabilities)

We assume a two-dimensional flow upstream of the impeller, as shown in Fig. 2. The length of the suction conduit, L, is assumed to be much larger than the wavelength s. We consider an axial flow with a uniform velocity U in the x direction and rotating blades with a constant velocity of U_T in the y direction as shown in Fig. 2. A stationary frame is used for this analysis. If the flowfield upstream of the impeller is assumed to be irrotational, the disturbances produced by flow instabilities are expressed by the following velocity potential:

$$\phi = (s/2\pi)\tilde{u}_1 \exp 2\pi j[nt - (y/s)] \exp[(2\pi/s)x] \qquad (1)$$

where s, n, and j are the wavelength in the y direction, the frequency, and the imaginary unit, respectively. Real parts are considered to have physical meanings throughout the present paper. The velocities u and v in the x and y directions are written as

$$u = U + \frac{\partial \phi}{\partial y} = U + \tilde{u}_1 \exp 2\pi j \left(nt - \frac{y}{s} \right) \exp \left(\frac{2\pi}{s}x \right)$$

$$v = \frac{\partial \phi}{\partial y} = -j\tilde{u}_1 \exp 2\pi j \left(nt - \frac{y}{s} \right) \exp \left(\frac{2\pi}{s}x \right) \qquad (2)$$

where the amplitude of fluctuating velocity $\tilde{u}_1$ is assumed to be much smaller than the uniform velocity U. The linearized momentum equation is written as

$$\frac{\partial u}{\partial t} + U\frac{\partial u}{\partial x} = -\frac{1}{\rho}\frac{\partial p}{\partial x} \qquad (3)$$
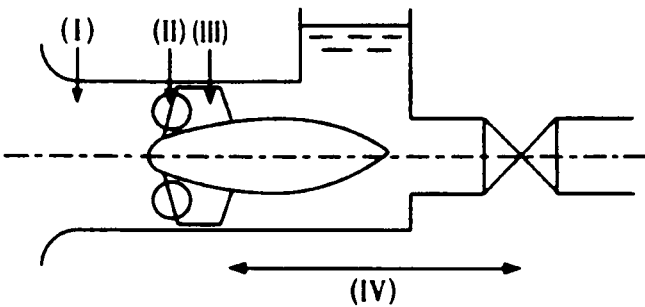

Fig. 1 Components of the turbomachine system: I, flow upstream of the impeller; II, cavitation at pump inlet; III, flow in the impeller; and IV, flow downstream of the impeller.
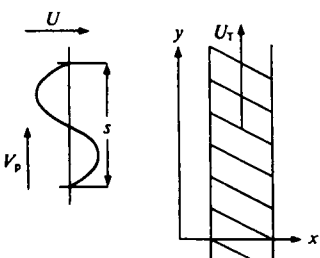

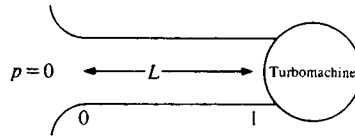Fig. 2 Flows upstream and downstream of impeller.

Fig. 3 One dimensional flow in suction conduit.

Substituting Eq. (2) into the preceding expression, we obtain the following fluctuating pressure field:

$$\delta p_1 = -\rho U(1 + jk)\tilde{u}_1 \exp 2\pi j[nt - y/s] \exp[(2\pi/s)x] \qquad (4)$$

where $k \equiv sn/U$ is the nondimensional reduced freqency. In general, k is complex and expressed by $k = k_R + jk_I$, and the following relations are used:

$$\exp 2\pi j (nt - y/s) = \exp[-2\pi (U/s)k_I t]$$

$$\times \exp 2\pi j (U/s)k_R(t - y/Uk_R)$$

$$V_p \equiv Uk_R = U_T(k_R/\tan\beta_1), \qquad \tan\bar{\beta}_1 \equiv U_T/U = 1/\phi$$

The quantities $k_R/\tan\bar{\beta}_1$ and k_I present the dimensionless propagating velocity in the y direction, Vp/U_T, and the damping rate, respectively. Then, in summary, if the amplitude of fluctuating velocity $\tilde{u}_1$ is given in the flowfield upstream of the turbomachine, the whole fluctuating flowfield is completely determined by Eqs. (2) and (4).

Surge Case and Cavitation Surge Case (One-Dimensional Instability)

We consider that the fluid flows from a space with constant pressure ($p = 0$) to a turbomachine through a conduit with a length of L, as shown in Fig. 3. The fluid velocities are denoted by

$$u = U + \tilde{u}_1 \exp 2\pi nt, \qquad v = 0 \qquad (5)$$

Applying Bernoulli's equation between positions 0 and 1 in Fig. 3, the pressure fluctuation at position 0, that is δp_0, is written as

$$\delta p_0 = -\rho U \tilde{u}_1 \exp 2\pi jnt$$

Integrating the momentum equation (3) from point 0 to 1 using Eq. (5), we obtain the following relation:

$$2\pi jnL\tilde{u}_1 \exp 2\pi jnt = -(1/\rho)(\delta p_1 - \delta p_0)$$

From the two expressions just described, the suction pressure δp_1 of the impeller will then be given by

$$\delta p_1 = -\rho U(1 + jk_L)\tilde{u}_1 \exp 2\pi jnt \qquad (6)$$

where $k_L \equiv 2\pi nL/U$ is the reduced frequency. If the fluctuating amplitude $\tilde{u}_1$ is given at the inlet of the impeller, the flowfield there can be completely prescribed by Eqs. (5) and (6). Equations (4) and (6) are very similar to each other, being expressions for the pressure at the inlet to the turbomachines obtained from the momentum equation.

Cavitation

Figure 4 shows the velocity triangle at the impeller inlet, cavitation, and the flow within the blades. The cavity volume V_c per blade and per unit span is normalized using the blade spacing h,

$$a(\sigma_1, \alpha_1) \equiv V_c/(h^2 \times 1) \qquad (7)$$

Under quasi-steady conditions, the nondimensional cavity volume a is considered to be a function of the incident angle α_1, and the cavitation number σ_1 is defined as follows:

$$\sigma_1 = \frac{p_1 - p_v}{\rho W_1^2/2} \qquad (8)$$

where p_1, p_v, and W_1 are the inlet pressure, the vapor pressure, and the relative velocity, respectively.
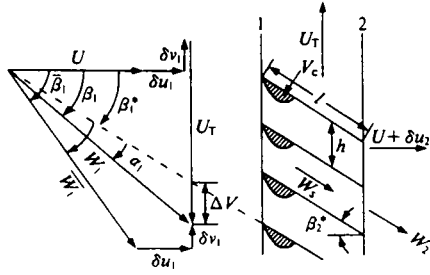
Fig. 4   Velocity triangle and cavitation at impeller inlet and flows in suction conduit.

Then, as originally suggested by Brennen and Acosta,[9] the change of cavity volume, δV_c, is related to the deviations δW_1, δa, and $\delta\sigma_1$ by

$$\delta V_c = h^2\left[\frac{\partial a}{\partial \sigma_1}\left(\frac{\partial \sigma_1}{\partial W_1}\delta W_1 + \frac{\partial \sigma_1}{\partial p_1}\delta p_1\right) + \left(\frac{\partial a}{\partial \alpha_1}\right)\delta\alpha_1\right] \quad (9)$$

From the velocity triangle shown in Fig. 4, the deviations δW_1 and $\delta\alpha_1$ can be expressed in terms of the deviations of δu_1 and δv_1 from the uniform axial velocity. Then Eq. (9) may be written as

$$\delta V_c = h^2\left[F_1(\delta u_1/U) + F_2(\delta v_1/U) + F_3\left(\delta p_1\big/\rho U^2\right)\right] \quad (10)$$

where

$$F_1 = 2\sigma \cos^2\bar\beta_1 K - \sin\bar\beta_1\cos\bar\beta_1 M$$

$$F_2 = -2\sigma\sin\bar\beta_1\cos\bar\beta_1 K - \cos^2\bar\beta_1 M, \qquad F_3 = -2\cos^2\bar\beta_1 K$$

$$(10')$$

$$M \equiv \frac{\partial a}{\partial\alpha_1}, \qquad K \equiv -\frac{\partial a}{\partial\sigma_1} \quad (11)$$

M and K are the mass flow gain factor and cavitation compliance, respectively.[1,9,10]
The continuity relation across the impeller is

$$h(\delta u_2 - \delta u_1) = \frac{\partial^*}{\partial t^*}\delta V_c \quad (12)$$

where $\partial^*/\partial t^*$ indicates the time differential in a frame fixed to the impeller and is expressed by the following form using Eqs. (2) and (5), for two-dimensional fluctuations:

$$\frac{\partial^*}{\partial t^*} = \frac{\partial}{\partial t} + U_T\frac{\partial}{\partial y} = 2\pi jn - U_T\frac{2\pi}{s}j = 2\pi j\frac{U}{s}(k - \tan\bar\beta_1)$$

and for one-dimensional fluctuations:

$$\frac{\partial^*}{\partial t^*} = \frac{\partial}{\partial t} + U_T\frac{\partial}{\partial y} = 2\pi jn = j\left(\frac{U}{L}\right)k_L$$

From Eqs. (10) and (12), we obtained the following equations that express the influence of the change of cavity volume for two-dimensional fluctuations:

$$\delta u_2 - \delta u_1 = 2\pi j(h/s)(k - \tan\bar\beta_1)U\left[F_1(\delta u_1/U)\right.$$

$$\left. + F_2(\delta v_1/U) + F_3\left(\delta p_1\big/\rho U^2\right)\right] \quad (13)$$

and for one-dimensional fluctuations:

$$\delta u_2 - \delta u_1 = j(h/L)k_L U\left[F_1(\delta u_1/U) + F_3\left(\delta p_1\big/\rho U^2\right)\right] \quad (14)$$
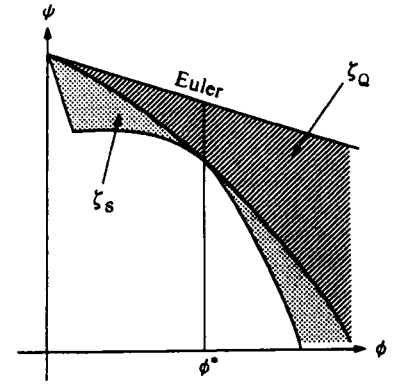

Fig. 5   Characteristics of impeller and assumptions of losses.

Pressure Rise in the Impeller

It is assumed that all of the cavitation can be lumped into the volume V_c, upstream of the blade passage, and that the subsequent impeller flow can be modeled as single-phase incompressible liquid flow (the more complex blade passage model of Brennen[11] suggests that this is a good first approximation). Then the unsteady Bernoulli's equation applied to the flow in the impeller (see Figs. 1 and 4) yields

$$\frac{p_2 - p_1}{\rho} = \frac{1}{2}\left(W_1^2 - W_2^2\right) - \frac{\partial^*}{\partial t^*}(\phi_2 - \phi_1) \quad (15)$$

If β^* is the average blade angle, as shown in Fig. 4, the difference of the velocity potential can be approximated by

$$\phi_2 - \phi_1 = \int_1^2 W_s\,ds \cong \frac{u_2\ell}{\cos\beta^*}$$

where subscripts 1 and 2 indicate the inlet and outlet of impeller and β^* is the mean blade angle. The total pressure loss in the impeller is represented by two coefficients, ζ_Q and ζ_S, where

$$\Delta p_t/\rho = \zeta_Q(U + \delta u_1)^2 + \zeta_S(\Delta V)^2 \quad (16)$$

and ΔV is the incident velocity as shown in Fig. 4. Thus, ζ_Q is the hydraulic loss in the blade passage, and ζ_S is the incidence loss at inlet as shown graphically in Fig. 5. Note that

$$\Delta V = (U + \delta u_1)\left(\tan\bar\beta_1 - \tan\beta_1^*\right)$$

The differences between pressure fluctuations upstream and downstream of the impeller are obtained by combining Eqs. (15) and (16) after linearization to yield

$$\frac{\delta p_2 - \delta p_1}{\rho U^2} = (1 - L_u)\frac{\delta u_1}{U} - (\tan\bar\beta_1 + L_v)\frac{\delta v_1}{U} - \frac{1}{\cos^2\beta_2^*}\frac{\delta u_2}{U}$$

$$- \begin{cases} \dfrac{1}{\cos\beta^*}jk_L\dfrac{l}{L}\dfrac{\delta u_2}{U} & \text{(for one-dimensional fluctuations)} \\[2ex] \dfrac{2\pi}{\cos\beta^*}j(k - \tan\bar\beta_1)\dfrac{\ell}{s}\dfrac{\delta u_2}{U} & \text{(for two-dimensional fluctuations)} \end{cases}$$

$$(17)$$

where L_u and L_v are given by

$$L_u = \frac{\partial\Delta p_t}{\partial(\rho U u_1)} = 2\zeta_Q + 2\zeta_S\tan\beta_1^*\left(\tan\beta_1^* - \tan\bar\beta_1\right)$$

$$L_v = \frac{\partial\Delta p_t}{\partial(\rho U v_1)} = 2\zeta_S\left(\tan\beta_1^* - \tan\bar\beta_1\right) \quad (18)$$

In general, flow instabilities in pumps appear at larger cavitation numbers than those which bring about significant deterioration in the pump performance. Therefore, for simplicity, the effect of cavitation on the pressure rise across the impeller has been omitted from the present analysis and is not included in Eq. (17).

Flowfield Downstream of the Impeller

In unsteady flow, the circulation of the impeller fluctuates with time, and free vorticity is shed from the impeller. Thus, the flow downstream of the impeller is rotational and can be represented by the combination of a potential disturbance, Eq. (1), and a disturbance due to the free vorticity. Here, however, we employ simpler flow models downstream of the impeller appropriate for each instability.

One-Dimensional Instabilities (Surge and Cavitation Surge)

Surge

When the outlet of the impeller is directly connected to a tank and the flow from the tank is discharged to a space of constant pressure through a valve as shown in Fig. 6, the continuity requires that

$$\delta u_2 - \delta u_3 = \frac{A}{\rho g f}\frac{d\delta p_2}{dt} = Cj\frac{U}{L}k_L\delta p_2 \tag{19}$$

where f and A are the cross-sectional areas of the conduit and the tank and $C(= A/\rho g f)$ is the compliance of the tank. For compressors, C is given by $V/(\rho a^2 f)$, where V is the volume of the tank and a is the speed of sound. The valve downstream of the tank is assumed to have the following characteristic:

$$\delta p_2/\rho U^2 = R(\delta u_3/U) \tag{20}$$

where R is the resistance of valve. From Eqs. (19) and (20), we obtain the following relations for the system consisting of the tank and the valve:

$$\delta u_2/U = \left(1/R + B^2\phi^2 jk_L\right)\left(\delta p_2/\rho U^2\right) \tag{21}$$

$$B = \sqrt{(\rho C/L)}U_T \tag{22}$$

where B is Greitzer's B factor,[3] which affects the occurrence of surge and the shape of the surge Lissajous.

We now proceed to put together the model for the one-dimensional instabilities, namely, surge and cavitation surge (formerly called auto-oscillation). The characteristics of the suction conduit are expressed by Eqs. (5) and (6). The characteristic of the cavitation is given by Eq. (14). If cavitation does not occur, $F_1 = 0$ and $F_3 = 0$ and Eq. (14) reduces to $\delta u_2 = \delta u_1$. The charactaristics of the impeller are expressed by Eq. (17). The characteristic of a tank and valve discharge system is expressed by Eq. (21). Substituting Eqs. (5), (6), (14), and (21) into Eq. (17) and eliminating unknowns other than δu_1, we obtain

$$\left[\frac{1}{(1/R) + B^2\theta^2 jk_L} + (1 + jk_L) - (1 - L_u)\right.$$

$$\left. + \frac{1}{\cos^2\beta_2^*} + \frac{1}{\cos\beta^*}\frac{l}{L}jk_L\right] \times \delta u_1 = 0 \tag{23}$$
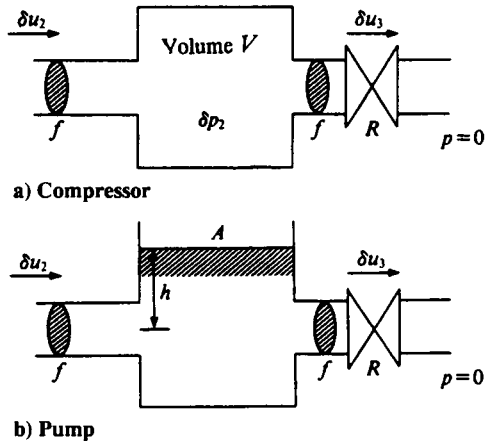

a) Compressor

b) Pump

Fig. 6 Tank-valve systems downstream of the impeller.

The portion inside the brackets in Eq. (23) must be zero for Eq. (23) to have a nontrivial solution. This yields the characteristic equation

$$B^2\phi^2\left[1 + \frac{1}{\cos\beta^*}\left(\frac{\ell}{L}\right)\right]k_L^2 - \left[\left\{1 + \frac{1}{\cos\beta^*}\left(\frac{\ell}{L}\right)\right\}\frac{1}{R}\right.$$

$$\left. + B^2\phi^2\left(L_u + \frac{1}{\cos^2\beta_2^*}\right)\right]jk_L - \left[1 + \frac{1}{R}\left(L_u + \frac{1}{\cos^2\beta_2^*}\right)\right] = 0 \tag{24}$$

which is a quadratic equation for jk_L with real coefficents. Two solutions of Eq. (24) are represented by

$$k_L = \pm k_R + jk_I \tag{25}$$

where k_R and k_I are the frequency and damping, respectively. Thus, the two solutions have the same frequency. Because k_I is zero and k_L is real in the case of neutral stability, the real part of Eq. (24) gives the following frequency:

$$n = \frac{U}{2\pi L}k_L \tag{26}$$

$$n = \frac{1}{2\pi}\frac{1}{\sqrt{\rho CL}}\sqrt{\frac{1 + (1/R)\left(L_u + 1/\cos^2\beta_2^*\right)}{1 + \ell/(L\cos\beta^*)}} \tag{27}$$

If the physical circumstances are such that $(L_u + 1/\cos^2\beta^*)/R \ll 1$ and $\ell/L \ll 1$, then the frequency is given by

$$n = (1/2\pi)\left(1/\sqrt{\rho CL}\right) \tag{28}$$

This is the natural frequency of a system that consists of the inlet conduit and the tank shown in Fig. 7.

The condition of neutral stability is obtained from the imaginary part of Eq. (24), namely,

$$L_u + \frac{1}{\cos^2\beta_2^*} = -\frac{1 + \ell/(L\cos\beta^*)}{B^2\phi^2 R} \tag{29}$$

downstream of the impeller. We employ the following impeller head rise coefficient using the total inlet pressure p_{t1} and the delivery static pressure p_2:

$$\psi_{ts} \equiv \frac{p_2 - p_{t1}}{\rho U_T^2} \tag{30}$$

Then the left-hand side of Eq. (29) may be written as

$$L_u + \frac{1}{\cos^2\beta_2^*} = -\frac{1}{\phi}\frac{\partial\psi_{ts}}{\partial\phi} \tag{29'}$$

Then the onset condition of surge $(k_I < 0)$ is given by

$$\frac{\partial\psi_{ts}}{\partial\phi} \geq \frac{1 + \ell/(L\cos\beta^*)}{B^2\phi R} \tag{31}$$

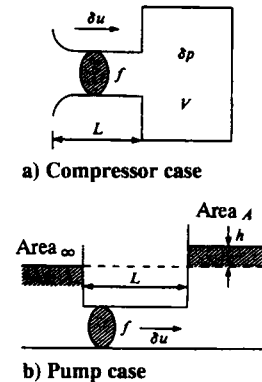a) Compressor case

b) Pump case

Fig. 7 Basic conduit system for surge.

Cavitation Surge

Some components with compliance must exist downstream of the impeller, or upstream of the impeller, or both for the usual surge to occur. However, cavitation surge does not require such components because the cavitation itself provides the compliance. Here we consider cavitation surge in which flow fluctuations do not occur downstream of the impeller. This would be the case if a very long conduit or a large resistance existed downstream of the impeller. Cavitation surge is analyzed as follows: The characteristics of the suction conduit are expressed by Eqs. (5) and (6). The characteristics of cavitation are expressed by Eq. (14). When it is assumed that $\delta u_2 = 0$ and Eqs. (5) and (6) are substituted into Eq. (14), the following equation is obtained:

$$[1 + jk_L(h/L)\{F_1 - (1 + jk_L)F_3\}](\delta u_1/U) = 0 \qquad (32)$$

This characteristic quadratic equation for jk_L has real coefficients. At neutral stability, the real part of Eq. (32) gives

$$n = \frac{U}{2\pi L}k_L = \frac{U}{2\pi L}\sqrt{-\frac{L}{hF_3}} = \frac{U_T}{2\pi}\frac{1}{\sin\bar{\beta}_1}\frac{1}{\sqrt{2KLh}} \qquad (33)$$

Thus the frequency of cavitation surge is proportional to the rotational speed of the impeller, whereas the frequency of surge given by Eq. (26) depends only on the characteristics of the conduit.

The dimensional compliance C, defined in Eq. (11), is expressed as follows for the system shown in Fig. 7:

$$\delta u = C\frac{d\delta p}{dt} \qquad (34)$$

The cavitation compliance K is related to the dimensional compliance C by Eqs. (10') and (14) so that

$$C = -\frac{F_3 h}{\rho U^2} = \frac{2\sin^2\bar{\beta}_1 h}{\rho U_T^2}\cdot K \qquad (35)$$

and using Eqs. (28) and (35), the frequency n becomes

$$n = \frac{1}{2\pi}\frac{1}{\sqrt{\rho CL}} = \frac{U_T}{2\pi}\frac{1}{\sin\bar{\beta}_1\sqrt{2KLh}}$$

This frequency is identical to that of Eq. (33). That the frequency of cavitation surge is proportional to the rotational speed of the impeller is because the compliance given by Eq. (35) is inversely proportional to U_T^2.

The onset condition for cavitation surge is obtained from the imaginary part of Eq. (32): $F_1 = F_3$, which further reduces to

$$M \geq 2(1 + \sigma)\phi K \qquad (36)$$

The sign of inequality in Eq. (36) is deduced from that k_L must have a small negative imaginary part for the instability to grow. Mass flow gain factor M and cavitation compliance K are, therefore, key quantities in determining the stability boundary. Because the cavity volume a usually increases with the increase of the attack angle α_1, the mass flow gain factor usually has a positive sign, and this tends to promote instability.

The destabilizing effect of the positive mass flow gain factor can be physically explained as follows: When the flow rate increases at the inlet, the incidence angle α decreases. If the mass flow gain factor is positive, the cavity volume decreases and the flow rate further increases at the inlet to fill up the decreased cavity volume.

The cavitation compliance is also positive because the cavity volume decreases with the increase of pressure, and this promotes system stability. Thus, the onset criterion represented by Eq. (36) indicates that cavitation surge appears when the destabilizing effect of the mass flow gain factor is stronger than the stabilizing effect of the cavitation compliance. Note that cavitation surge can occur independently of the form of the head rise/flow rate performance characteristic and, in this regard, is very different from regular surge.

Two-Dimensional Instabilities (Rotating Stall and Rotating Cavitation)

Rotating stall

For the sake of simplicity, it is assumed that the flow is delivered from the impeller to a reservoir in which the pressure is constant. The characteristics of the flow upstream of the impeller are given by the following relations using Eqs. (2) and (4):

$$\delta u_1 = \tilde{u}_1\exp 2\pi j(nt - y/s), \qquad \delta v_1 = -j\tilde{u}_1\exp 2\pi j(nt - y/s) \qquad (2')$$

$$\delta p_1 = -\rho U(1 + jk)\tilde{u}_1\exp 2\pi j(nt - y/s) \qquad (4')$$

The continuity equation that neglects the effect of cavitation compliance so that $\delta V_c = 0$ follows from Eq. (12):

$$\delta u_2 = \delta u_1 \qquad (12')$$

The pressure rise across the impeller is given by Eq. (17):

$$\frac{\delta p_2 - \delta p_1}{\rho U^2} = (1 - L_u)\frac{\delta u_1}{U} - (\tan\bar{\beta}_1 + L_v)\frac{\delta v_1}{U}$$

$$-\frac{1}{\cos^2\beta_2^*}\frac{\delta u_2}{U} - \frac{2\pi}{\cos\beta^*}j(k - \tan\bar{\beta}_1)\frac{\ell}{s}\frac{\delta u_2}{U} \qquad (17')$$

Because the flow is delivered to the constant pressure reservoir,

$$\delta p_2 = 0 \qquad (37)$$

Substituting Eqs. (2'), (4'), (12'), and (37) into Eq. (17') produces

$$\left[\left\{1 - L_u - \left(1/\cos^2\beta_2^*\right) - (2\pi j/\cos\beta^*)(l/s)(k - \tan\bar{\beta}_1)\right\}\right.$$

$$\left. - (1 + jk) + j(\tan\bar{\beta}_1 + L_v)\right](\delta u_1/U) = 0 \qquad (38)$$

Thus, the characteristic equation is linear in k. Substituting $k = k_R + jk_I$, we obtain the following relations for the real and imaginary parts:

$$k_I = \frac{L_u + 1/\cos^2\beta^*}{1 + 2\pi\ell/(s\cdot\cos\beta^*)} = -\frac{\partial\psi_{ts}/\partial\phi}{1 + 2\pi\ell/(s\cdot\cos\beta^*)}\frac{1}{\phi} \qquad (39)$$

$$\frac{V_p}{U_T} = \frac{k_R}{\tan\bar{\beta}_1} = 1 - \frac{2\zeta_s(1 - \phi/\phi^*)}{1 + 2\pi\ell/(s\cdot\cos\beta^*)} \qquad (40)$$

Because k_I is the damping rate of disturbance, the onset condition of rotating stall is given by

$$\frac{\partial\psi_{ts}}{\partial\phi} > 0 \qquad (41)$$

Equation (41) states that rotating stall occurs if the curve of the pressure rise of impeller (calculated using the outlet static pressure and inlet total pressure) has a positive slope. This result is precisely the conventional one described by Greitzer.[2] By comparison of Eqs. (41) and (31), it is clear that rotating stall occurs more easily than surge. Because the flow coefficient $\phi(= \cot\bar{\beta}_1 = U/U_T)$ satisfying Eq. (41) is generally less than the incidence free-flow coefficient $\phi^*(= \cot\beta_1^*)$, Eq. (40) yields $V_P/U_T < 1$, which indicates that the stalled region propagates with an angular speed lower than that of the rotating impeller.

Note that Eq. (41) was obtained under the assumption that the impeller discharged to a constant pressure reservoir. Altenatively, if the flow downstream were semi-infinite and two dimensional, the term $1 + (2\pi/\cos\beta^*)(\ell/s)$ in Eqs. (39) and (40) would be replaced by $[2 + (2\pi/\cos\beta^*)(\ell/s)]$.

Rotating Cavitation

As with cavitation surge, we consider the circumstance in which there are no velocity fluctuations downstream of the impeller. This would occur when the chord length of the impeller is large or the outlet blade angle is near 90 deg. These conditions would imply a large fluid inertia in the impeller and a large negative slope of the pressure performance of the impeller. These in turn would suppress the flow fluctuations downstream of the impeller.

When Eqs. (2) and (4) are used, the characteristics of the flow upstream of the impeller are given by

$$\delta u_1 = \widetilde{u_1} e z p 2\pi j (nt - u/s), \qquad \delta v_1 = -j\widetilde{u_1} \exp 2\pi j (nt - y/s)$$

(2')

$$\delta p_1 = -\rho U (1 + jk)\widetilde{u_1} \exp 2\pi j (nt - y/s)$$

(4')

The cavitation characteristics are expressed by Eq. (13):

$$\delta u_2 - \delta u_1 = 2\pi j (h/s)(k - \tan \bar{\beta}_1) U$$

$$\times \left[F_1(\delta u_1/U) + F_2(\delta v_1/U) + F_3\left(\delta p_1\Big/\rho U^2\right) \right]$$

(13')

When $\delta u_2 = 0$ is assumed and Eqs. (2') and (4') are substituted into Eq. (13'), the following equation is obtained:

$$[1 + 2\pi j (h/s)(k - \tan \bar{\beta}_1)\{F_1 - jF_2 - (1 + jk)F_3\}](\delta u_1/U) = 0$$

(42)

and this results in a quadratic characteristic equation for k. The onset condition for rotating cavitation is then

$$M \geq 2(1 + \sigma)\phi K$$

(43)

Equation (43) is identical to Eq. (36) for the onset condition of cavitation surge.

The occurrence of rotating cavitation can be explained by almost the same argument as cavitation surge. For rotating cavitation, we simply need to consider the increase of flow rate at a specific circumferential location. Therefore, rotating cavitation can be considered to be a two-dimensional instability that is caused by the destabilizing effect of the mass flow gain factor. As with cavitation surge, rotating cavitation can occur even at a design point, independently of the flow rate and the characteristics of the impeller. This feature of rotating cavitation is quite different from that of rotating stall. From the real part of Eq. (42), we obtain the following relation:

$$(k - \tan \bar{\beta}_1)(k + F_2/F_3) = -s/(2\pi h F_3)$$

(44)

When $V_p/V_T = k/ \tan \bar{\beta}_1$ and the expressions (10') of F_2 and F_3 are used, Eq. (44) may then be written in the following form:

$$(V_p/U_T - 1)\{V_p/U_T + (\sigma + M\phi/(2K))\} = (s/h)\left(4\pi K \sin^2 \bar{\beta}_1\right)$$

(45)

The two solutions of Eq. (45) have the following characteristics:

$$V_p/U_T > 1$$

(46)

$$V_p/U_T < -[\sigma + M\phi/(2K)]$$

(47)

Thus, rotating cavitation has two modes. One of them propagates faster than the impeller and the other propagates in the opposite direction. We term these forward and backward rotating cavitation, respectively. Earlier experimental results (for example, Kamijo et al.[12,13]) had noted the forward-rotating cavitation phenomenon. More recently, Hashimoto et al.[14] have also observed the backward form of rotating cavitation. It has not been clarified why forward-rotating cavitation is more often observed than backward-rotating

cavitation, although the onset condition of both modes are theoretically the same.

Mutual Relation of Flow Instabilities

Rotating Stall and Rotating Cavitation

In the preceding section, rotating stall and rotating cavitation were independently investigated. In this section, we consider the case in which they may coexist. In the preceding section, we used the condition $\delta u_1 = \delta u_2$ for rotating stall. The effect of cavitation can be easily included by replacing this relation with Eq. (13). Then, the characteristic equation becomes
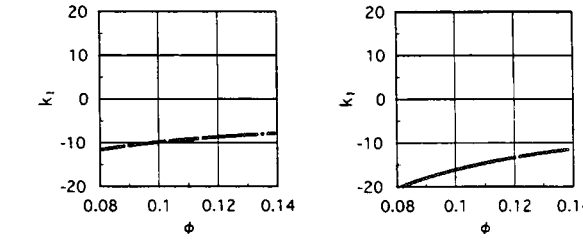

a)

b)   Equation (48)   Equation (24)

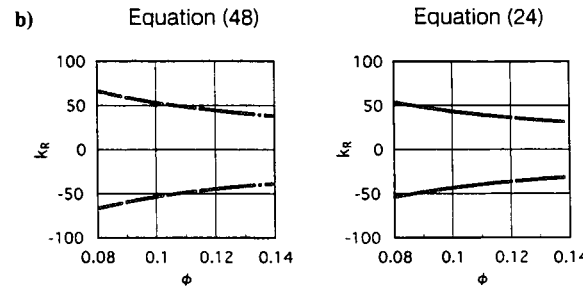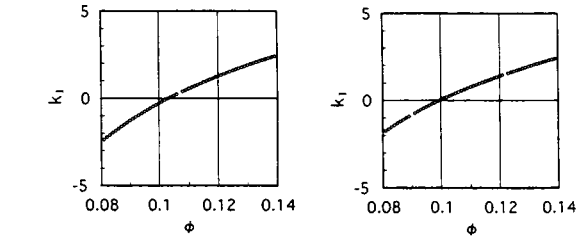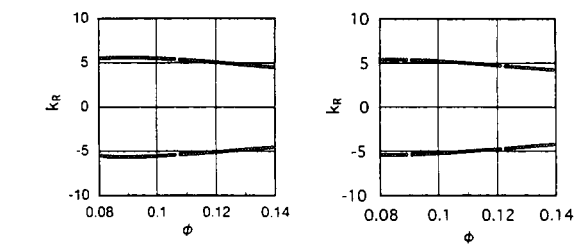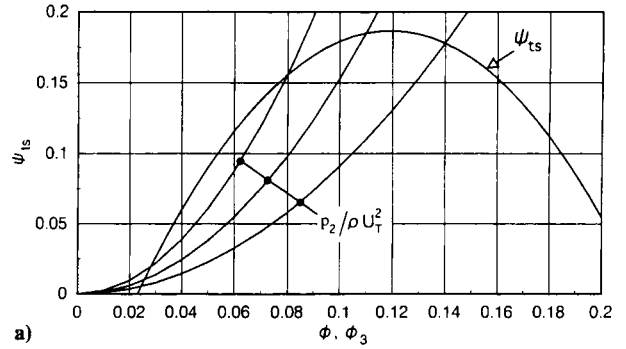c)   Equation (50)   Equation (32)

Fig. 8 Comparisons of the root of Eq. (50) (surge + cavitation surge) with those of Eqs. (23) (surge) and (32) (cavitation surge), where B = 1.0, ℓ/L = 1.0, β_2^* = β = 76 deg, ζ_Q = 2.0, and ζ_s = 0.6; R is determined from the parabolic resistance curve for $/p_2/\rho U_T^2 \sim \phi_3 \equiv u_3/U_T$ shown in a) performance curve, b) conventional surge, and c) cavitation surge.

$$\left\{1\Big/\cos^2\beta_2^* + (2\pi/\cos\beta^*)(\ell/s)(k - \tan\bar\beta_1)j\right\}[1 + 2\pi j(h/s)(k$$

$$- \tan\bar\beta_1)\{F_1 - jF_2 - (1 + jk)F_3\}]$$

$$+ j(k - \tan\bar\beta_1) - jL_v + L_u = 0 \qquad (48)$$

As before, this is based on the assumption that the the impeller discharges to a constant pressure reservoir. When it is assumed that a two-dimensional flow continues downstream of the impeller, the term $(2\pi/\cos\beta^*)(\ell/s)$ is replaced by $[1 + (2\pi/\cos\beta^*)(\ell/s)]$ in Eq. (48). Then if $\beta_2^* \to 90$ deg or $\ell/s \to \infty$, Eq. (48) becomes

$$1 + 2\pi j(h/s)(k - \tan\bar\beta_1)\{F_1 - jF_2 - (1 + jk)F_3\} = 0 \qquad (49)$$

This is identical to Eq. (42), the result for rotating cavitation. This can be explained as follows. The negative slope of the head-capacity curve becomes infinite in the limit of $\beta_2^* \to 90$ deg, and the inertia of the fluid within the impeller also becomes infinite in the limit of $\ell/s \to \infty$, and this results in $\delta u_2 \to 0$. Rotating stall is suppressed due to the condition $\delta u_2 = 0$. When the influence of cavitation is extremely small, F_1, F_2, and F_3 approach zero. In this case, Eq. (48) agrees with Eq. (37), the result for rotating stall.

When rotating stall and rotating cavitation coexist, Eq. (48) must be solved, and it is cubic in k. When the equation is solved with the assumption of two-dimensional flow downstream of the impeller, the following three solutions of k are obtained:

$$(V_p/U_t)_1 = \text{Real}(k_1/\tan\bar\beta_1) > 1$$

$$(V_p/U_t)_2 = \text{Real}(k_2/\tan\bar\beta_1) < 0$$

$$(V_p/U_t)_3 = \text{Real}(k_3/\tan\bar\beta_1) < 1$$

Furthermore, the following interesting features of k_1, k_2, and k_3 emerge:
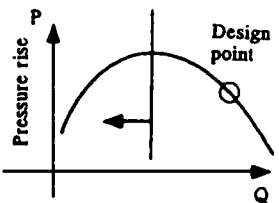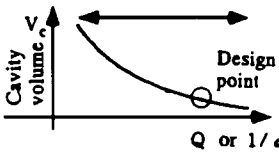
Table 1   Flow instabilities of turbomachines

Cause and flow regions of occurrence	One-dimensional flow instabilities	Two-dimensional and local flow instabilities
	Surge	Rotating stall
	Cavitation surge	Rotating cavitation

1) The values of k_1 and k_2 are close to those obtained by Eq. (45), that is, k_1 and k_2 represent rotating cavitation. On the other hand, the value of k_3 is close to that from Eq. (38), showing that k_3 represents rotating stall.

2) The value of k_3 depends on the flow coefficient ϕ and loss coefficients, ζ_Q and ζ_s, whereas the influence of these coefficients on k_1 and k_2 is small.

3) The mass flow gain factor M and the cavitation compliance K have a substantial influence on k_1 and k_2, but not on k_3.

The roots, k_1, k_2, and k_3, can coexist, amplify, and damp independently of each other, which indicates that rotating cavitation and rotating stall are independent phenomena. Most interestingly, Murai[15] observed rotating stall with cavitation (the k_3 root) in experiments on an axial-flow pump.

Surge and Cavitation Surge

As in the preceding section, we can investigate the case of coexistence of surge and cavitation surge by replacing the relation of $\delta u_2 = \delta u_1$ with Eq. (14) in the surge analysis. Then, the characteristic equation becomes

$$\left(\frac{1}{1/R + B^2\phi^2 jk_L} + \frac{1}{\cos^2\beta_2^*} + \frac{1}{\cos\beta^*}\frac{\ell}{L}jk_L\right)\left[1 + \frac{h}{L}jk_L\{F_1\right.$$

$$\left. -(1 + jk_L)F_3\}\right] + jk_L + L_u = 0 \qquad (50)$$

When β_2^* approaches 90 deg or ℓ/L becomes infinite, Eq. (50) yields Eq. (32) for cavitation surge. When the influence of cavitation is extremely small, F_1 and F_3 are negligible, and Eq. (50) reduces to Eq. (23) for surge. Because Eq. (50) is a biquadratic equation with real coefficients for jk_L, there are two sets of complex conjugate solutions for jk_L, that is, $a_{1,2} \pm b_{1,2}j$. Therfore, k_L is expressed by $k_L = \pm b_{1,2} - ja_{1,2}$. Figure 8 shows the comparisons of the four roots of Eq. (50) with those of Eq. (23) for conventional surge (Fig. 8b) and with Eq. (32) for cavitation surge (Fig. 8c), for the performance curve shown in Fig. 8a. This clearly shows that Eq. (50) has two types of roots corresponding to conventional surge and cavitation surge and that the simplifications made for the derivations of Eqs. (23) and (32) do not largely affect the results. We observe that the surge (Fig. 8b) becomes stabilizing ($k_I > 0$) as we increase the flow coefficient ϕ whereas the cavitation surge (Fig. 8c) keeps amplifying ($k_I < 0$). Similar plots against M show that the stability k_I of cavitation surge largely depends on the value of M, whereas the surge is almost independent on the value of M.

Tables 1 and 2 show the onset conditions and frequencies of the four flow instabilities in turbomachines that were obtained by the present linear analysis.

Conclusions

1) Surge and rotating stall are one- or two-dimensional flow instabilities caused by a positive slope of the head-capacity curve.

2) Cavitation surge and rotating cavitation are also one- or two-dimensional flow instabilities caused by a positive mass flow gain factor M.

3) The frequency of surge depends substantially on the characteristics of the system. The rotating frequency of rotating stall depends

Table 2   Onset conditions and frequencies of flow instabilities of turbomachines

Instability	Onset condition	Frequency
Surge	$\dfrac{\partial\psi_{ts}}{\partial\phi} > \dfrac{1 + (1/\cos\beta^*)(l/L)}{B^2\phi R}$	$n = \dfrac{1}{2\pi}\dfrac{1}{\sqrt{\rho CL}}\sqrt{\dfrac{1 + (1/R)\left[L_u + \left(1\big/\cos^2\beta_2^*\right)\right]}{[1 + (1/\cos\beta^*)l/s]}}$
Rotating stall	$\dfrac{\partial\psi_{ts}}{\partial\phi} > 0$	$\dfrac{V_p}{U_T} = 1 - \dfrac{2\zeta_s[1 - (\phi/\phi^*)]}{1 + (2\pi/\cos\beta_1)l/s} < 1$
Cavitation surge	$M > 2(1 + \sigma)\phi K$	$n = \dfrac{U_r}{2\pi}\dfrac{1}{\sin\bar\beta_1}\dfrac{1}{\sqrt{2KLh}}$
Rotating cavitation	$M > 2(1 + \sigma)\phi K$	$V_p/U_T > 1,\quad V_p/U_T < 0$

on the performance and geometry of the impeller. It is proportional to and smaller than the rotational speed of the impeller.

4) The frequency of cavitation surge and the rotating frequency of rotating cavitation are proportional to the rotational speed of the impeller. The frequency of cavitation surge is the frequency of a system with the compliance provided by the cavitation. The rotating frequency of rotating cavitation depends on the geometry and cavitation characteristics of the impeller. Rotating cavitation has two modes: One propagates faster than the impeller and the other propagates in the opposite direction to the impeller.

References

[1] Brennen, C. E., *Hydrodynamics of Pumps*, Oxford Univ. Press and Concepts ETI, Inc., Oxford, England, U. K., 1994.

[2] Greitzer, E. M., "Surge and Rotating Stall in Axial Flow Compressors, Part 1—Theoretical Compression System Model," *Journal of Engineering for Power*, Vol. 98, No. 2, 1976, pp. 190–198.

[3] Greitzer, E. M., "Surge and Rotating Stall in Axial Flow Compressor: Part 2—Experimental Results and Comparison with Theory," *Journal of Engineering for Power*, Vol. 98, No. 2, 1976, pp. 199–217.

[4] Cumpty, N. A., and Greizer, E. M., "A Simple Model for Compressor Stall Cell Propagation," *Journal of Engineering for Power*, Vol. 104, No. 1, 1982, pp. 170–176.

[5] Moore, F. K., "A Theory of Rotating Stall of Multistage Axial Compressors:Part I—Small Disturbances," *Journal of Engineering for Gas Turbines and Power*, Vol. 106, No. 2, 1984, pp. 313–336.

[6] Moore, F. K., and Greizer, E. M., "A Theory of Post-Stall Transients in Axial Compression Systems:Part II—Application," *Journal of Engineering for Gas Turbines and Power*, Vol. 108, No. 2, 1986, pp. 231–239.

[7] Hynes,T. P., and Greizer, E. M., "A Metod for Assesing Effects of Inlet Flow Distortion on Compressor Stability," *Journal of Turbomachinery*, Vol. 109, No. 3, 1987, pp. 371–379.

[8] Tsujimoto, Y., Kamijo, K., and Yoshida, Y., "A Theoretical Analysis of Rotating Cavitation in Inducers," *Journal of Fluids Engineering*, Vol. 115, No. 1, 1993, pp. 135–141.

[9] Brennen, C., and Acosta, A. J., "The Dynamic Transfer Function for a Cavitating Inducer," *Journal of Fluids Engineering*, Vol. 98, No. 2, 1976, pp. 182–191.

[10] Ng, S. L., and Brennen, C., "Experiments on the Dynamic Behavior of Cavitating Pumps," *Journal of Fluids Engineering*, Vol. 100, No. 2, 1978, pp. 166–176.

[11] Brennen, C., "The Bubbly Flow Model for the Dynamic Characteristics of Cavitating Pump," *Journal of Fluids Mechanics*, Vol. 89, No. 2, 1978, pp. 223–240.

[12] Kamijo, K., Shimura, T., and Watanabe, M., "A Visual Observation of Cavitating Inducers," American Society of Mechanical Engineers, ASME Paper 77-WA/FE-14, Nov. 1977; also NAL Rept. TR-598T, 1980.

[13] Kamijo, K., Yoshida, M., and Tsujimoto, Y., "Hydraulic and Mechanical Performance of LE-7 LOX Pump Inducer," *Journal of Propulsion and Power*, Vol. 9, No. 6, 1993, pp. 819–826.

[14] Hashimoto, T., Yoshida, M., Watanabe, M., Kamijo, K., and Tsujimoto, Y., "Experimental Study on Rotating Cavitation of Rocket Propellant Pump Inducers," *Journal of Propulsion and Power*, Vol. 13, No. 4, 1997, pp. 488–494.

[15] Murai, H., "Observations of Cavitation and Flow Patterns in an Axial Flow Pump at Low Flow Rate," *Mem. Inst. High Speed Mech*, Vol. 24, No. 246, 1968/1969, pp. 315–333 (in Japanese).